ADVANCED MATERIALS
www.advmat.de

Zero Linear Compressibility in Nondense Borates with a "Lu-Ban Stool"-Like Structure

*Xingxing Jiang, Yi Yang, Maxim S. Molokeev, Pifu Gong, Fei Liang, Shuaihua Wang, Lei Liu, Xiang Wu, Xiaodong Li, Yanchun Li, Shaofan Wu, Wei Li, Yicheng Wu, and Zheshuai Lin**

Discovering materials that exhibit zero linear compressibility (ZLC) behavior under hydrostatic pressure is extremely difficult. To date, only a handful of ZLC materials have been found, and almost all of them are ultrahard materials with densified structures. Here, to explore ZLC in nondense materials, a structural model analogous to the structure of the "Lu-Ban stool," a product of traditional Chinese woodworking invented 2500 years ago, is proposed. The application of this model to borates leads to the discovery of ZLC in AEB_2O_4 (*AE* = Ca and Sr) with the unique "Lu-Ban stool"-like structure, which can obtain a subtle mechanical balance between pressure-induced expansion and contraction effects. Coupled with the very wide ultraviolet transparent windows, the ZLC behavior of AEB_2O_4 may result in some unique but important applications. The applications of the "Lu-Ban stool" model open a new route for pursuing ZLC materials in nondense structural systems.

Observations in our daily lives tell us that materials squeezed by hydrostatic pressure, that is, the force exerted by a fluid at static equilibrium, will always contract in all directions. In order to meet some special criterion of performance, however, this pressure-induced contraction should be avoided.[1–3] In some extreme cases, materials are required to remain constant in length along a specified direction,[4,5] that is, exhibiting zero linear compressibility (ZLC, or linear incompressibility) behavior under hydrostatic pressure.[6] The mechanical characteristic of ZLC materials goes against common physical sense, and will provide a unique solution for the key devices of precise instruments to maintain good stability under complicated environments within the pressure-fluctuation condition, such as functional preservation technology in marine bionics,[4] optical telecommunication apparatus, and ultrafine sensing system necessarily to be operated in deep sea,[1,7] and hence, the search for ZLC materials is highly desirable.

Linear compressibility, a measure of the relative length change of a solid as a response to a pressure change, is defined as $-\mathrm{d}L/L\mathrm{d}P$, where L is length and P is pressure.[2,8] Materials with an absolute magnitude of linear compressibility less than that of diamond (0.75 TPa^{-1}),[9] the hardest material in nature, can normally be regarded as ZLC materials.[6,10] In fact, the linear compressibility along the i-axis α_{ii} can also be deduced from the elastic

Dr. X. Jiang, Y. Yang, Dr. P. Gong, F. Liang, Prof. Z. Lin
Technical Institute of Physics and Chemistry
Chinese Academy of Sciences
Beijing 100190, China
E-mail: zslin@mail.ipc.ac.cn
Y. Yang, F. Liang, Prof. Z. Lin
University of Chinese Academy of Sciences
Beijing 100049, China
Dr. M. S. Molokeev
Laboratory of Crystal Physics
Kirensky Institute of Physics
Federal Research Center KSC SB RAS
Krasnoyarsk 660036, Russia
Dr. M. S. Molokeev
Department of Physics
Far Eastern State Transport University
Khabarovsk 680021, Russia
Dr. M. S. Molokeev
Siberian Federal University
Krasnoyarsk 660041, Russia
Dr. S. Wang, Prof. S. Wu
Fujian Institute of Research on the Structure of Matter
Chinese Academy of Sciences
Fuzhou, Fujian 350002, China
Dr. L. Liu
Mulliken Center for Theoretical Chemistry Institute for Physical and Theoretical Chemistry
University of Bonn
Bonn 53115, Germany
Prof. X. Wu
State Key Laboratory of Geological Processes and Mineral Resources
China University of Geosciences
Wuhan 430074, China
Dr. X. Li, Y. Li
Beijing Synchrotron Radiation Facility
Institute of High Energy Physics
Chinese Academy of Sciences
Beijing 100049, China
Prof. W. Li
School of Physics and Wuhan National High Magnetic Field Center
Huazhong University of Science and Technology
Wuhan 430074, China
Prof. Y. Wu
Institute of Functional Crystals
Tianjin University of Technology
Tianjin 300384, China

DOI: 10.1002/adma.201801313

compliance coefficient matrix (S) according to the formula $\alpha_{ii} = s_{ii} + s_{ij} + s_{ik}$, where the i-, j-, and k-axes are mutually perpendicular to each other. To clarify the underlying physics, the formula can also be expressed as $\alpha_{ii} = s_{ii}\,(1 - \nu_{ij} - \nu_{ik})$, where ν_{ij} is Poisson's ratio of the i-axis with respect to the j-axis. Accordingly, the compression of either of two ultimate mechanical limits, $s_{ii} \approx 0$ or $\nu_{ij} + \nu_{ik} \approx 1$, can result in the achievement of ZLC behavior. To date, the exploration of ZLC materials has been mainly concentrated on the materials with densified structures which have large resistance to external pressure, that is, $s_{ii} \approx 0$. This has led to the breakthrough discoveries of this rare mechanical behavior in some ultrahard materials with a very large Young's modulus, including osmium,[11] ReB_2,[6] and FeB_4.[12] By contrast, ZLC behavior in nondense materials has never been studied.

We notice that actually ZLC behavior in nondense materials can also be realized if the structural evolution satisfies the other condition, that is, $\nu_{ij} + \nu_{ik} \approx 1$. After some simple algebra, one may easily obtain that $\Delta\varepsilon_i \sim -\Delta\varepsilon_j - \Delta\varepsilon_k$, where $\Delta\varepsilon_i$, $\Delta\varepsilon_j$, and $\Delta\varepsilon_k$ are the strains along the i-, j-, and k-axes, respectively. This equation means that when compressed by axial stress, the structure that can equally (or losslessly) convert the pressure-induced axial strain to the perpendicular directions (while keeping the volume almost constant) will lead to ZLC behavior (**Figure 1**a), regardless of the degree of compactness of the structures. Compared with materials with densified structures, the nondense materials have their special superiority with a much larger repository of members and structural varieties as well as a high tunability of microstructures,[13] which would lead to some special applications if combined with the ZLC behavior.

An effective way of achieving strain conversion in a nondense material is to make the rigid constitutional units rotate with respect to the axial pressure such that the longitudinal strain can be effectively converted to the transverse strains. However, this does not guarantee that the strain conversion is lossless, and thus, the strains on some other microscopic units need to be subtly generated to compensate. Let us consider a 2D case in which the rigid unit (e.g., a bar) has an inclination angle θ ($0° < \theta < 45°$) with the i-axis initially. Under hydrostatic pressure conditions, as shown in Figure 1b, the angle between the bar and the i-axis will decrease by a degree of $\Delta\theta$. If $\Delta\theta$ is small, then the rotation of the bar results in the strain along the i-axis of $-\tan\theta\Delta\theta$, where the negative sign represents the negative linear compressibility. Therefore, the longitudinal strain of some other microscopic units with positive linear compressibility must be subtly "added" in order to achieve ZLC behavior along the i-axis in the material.

Accordingly, we herein propose that the linear compression in nondense materials under hydrostatic pressure can be effectively stopped when the microscopic units adopt a structural arrangement named after the "Lu-Ban stool", which is a 2500-year-old Chinese cultural heritage of woodworking. The Lu-Ban stool is made of a single piece of timber without any nails and consists of four rigid components (two legs and two planks serving as the faces). By adjusting the stool legs its architecture can be longitudinally transformed between a condensed wood block and an open-framework structure, which manifests a classic and famous model with a simplest mechanical structure to realize the balance of forces (see Figure 1c and Video S1, Supporting Information). Notably, the two planks of the "Lu-Ban stool" form a cross (with an angle θ to the longitudinal axis less than 45°), and as the hydrostatic pressure increases, their dihedral angle decreases and leads to negative compressibility along the longitudinal direction. If this anomalous expansion could be effectively cancelled out by the pressure-induced contraction of the stool legs along the longitudinal axis, then ZLC behavior would occur. In fact, in the "Lu-Ban stool" model, the mechanical behavior is considered only in a plane; thus, this model is quasi-2D. Meanwhile, the large interspace spanned by the legs creates a rigid unit with open space. The "Lu-Ban stool" structure therefore presents a simple but ideal prototype model to explore nondense ZLC materials. Interestingly, at the first glance the architecture of "Lu-Ban stool" is similar to that of "wine rack,"[8] a typical structure for negative compressibility which have already received a lot of attention. However, the detailed mechanism comparison reveals that, under the hydrostatic pressure, in the "wine rack" structures all components along the direction of negative compressibility are rigid, while in the "Lu-Ban stool"-like structures the negative compressibility resulted from the two planks is effectively counterbalanced by the positive compressibility of the two stool legs.

In particular, we apply the "Lu-Ban stool"-like model to the exploration of ZLC materials in the borate compounds since the boron–oxygen microscopic groups are kept nearly rigid under ambient mechanical or temperature disturbance.[14] Furthermore, due to the strong covalent interaction between boron and oxygen atoms, borates often possess wide bandgaps ($E_g > 6.22$ eV) with a transparent window down to the deep-ultraviolet (UV) region (wavelength $\lambda < 200$ nm).[15] Thus, if found, ZLC borates may realize applications in ultraprecise pressure–optics and pressure–electricity coupling devices, which urgently demand wide-bandgap materials.[1] Moreover, borate materials exhibit a large structural diversity since the BO_3 triangles and BO_4 tetrahedra presented in borates can be further interconnected to construct 1D, 2D, or 3D frameworks, leading to a large filtering space for suitable structure searching.[15]

Based on the above considerations, we noticed that the planar BO_3 triangles, if in a crossed manner with respect to one another, are analogous to the planks of "Lu-Ban stool". Meanwhile, the ionic bond interaction between alkali earth cations and oxygen ions is relatively sensitive to the ambient pressure which may play the role of the "stool legs" to compensate the negative compressibility from BO_3 "planks." Accordingly, we screened borate compounds in the Inorganic Crystal Structure Database (ICSD, 2017-2, Version 1.9.6, by Fachinformationszentrum Karlsruhe, Germany) and found that the borates of the form AEB2O4 (AE = Sr or Ca) possess a structural feature analogous to the "Lu-Ban stool" model. Additional in situ high-pressure X-ray diffraction (XRD) experiments (at the Beijing Synchrotron Radiation Facility) confirmed that AEB_2O_4 exhibits ZLC behavior between 0 and 8.0 GPa. The "Lu-Ban stool" model, combined with first-principles simulations, allowed the elucidation of the microscopic mechanism of their ZLC behavior. Moreover, AEB_2O_4 compounds possess a very wide bandgap of ≈7.2 eV. Owing to these properties, AEB_2O_4 may find potential applications in ultraprecise optical instruments used in complex environments. More importantly, our study

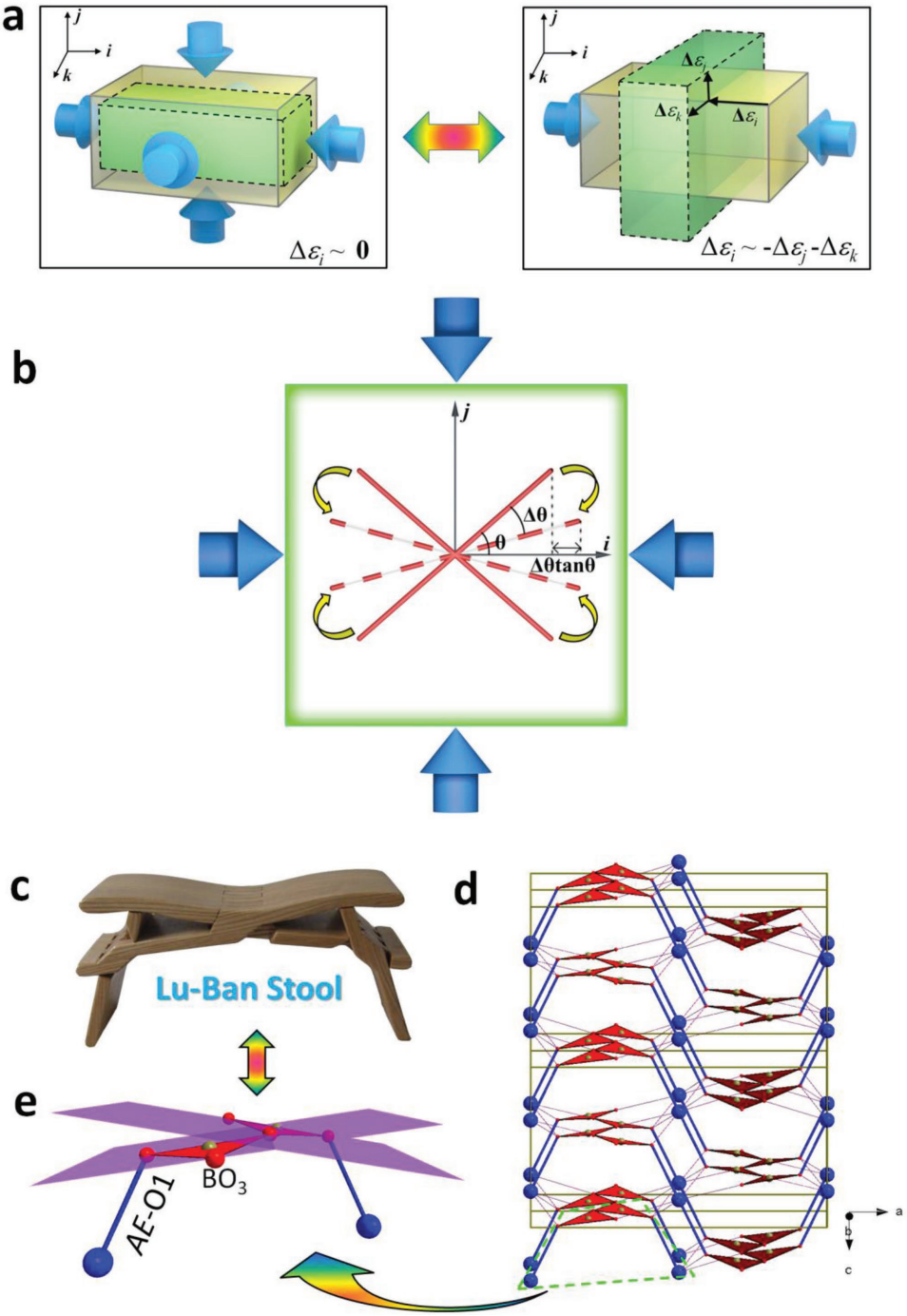

Figure 1. Mechanism of the ZLC effect in nondense materials, the "Lu-Ban stool" model, and the analogous structure in AEB_2O_4. a) ZLC behavior along the *i*-axis under hydrostatic pressure ($\Delta\varepsilon_i \approx 0$) is equivalent to the situation when Poisson's ratios $\nu_{ij} + \nu_{ik} \approx 1$ under axial pressure, that is, $\Delta\varepsilon_i \sim -\Delta\varepsilon_j - \Delta\varepsilon_k$, where $\Delta\varepsilon_i$, $\Delta\varepsilon_j$, and $\Delta\varepsilon_k$ are the strains along the *i*-, *j*-, and *k*-axes, respectively. The yellow and green boxes represent the initial and final states, respectively, as the pressure is applied. Note that under axial pressure, the volumes of ZLC materials remain nearly constant. b) Schematic of the structural response of a 2D rigid model to hydrostatic pressure. The length of the rigid bar is defined as 2*L*, and the inclination angle to the *i*-axis is θ ($0° < \theta < 45°$); hence, the projection on this axis is $L\cos\theta$. Under hydrostatic pressure, the angle between the bar and the *i*-axis decreases to $\theta - \Delta\theta$ ($\Delta\theta$ is a small quantity), and then the pressure-induced strain is $-[L\cos(\theta - \Delta\theta) - L\cos\theta]/L\cos\theta = -L\sin\theta\Delta\theta/L\cos\theta = -\tan\theta\Delta\theta$, which corresponds to negative compressibility. c) Configuration of a Lu-Ban stool. d) Crystal structure of AEB_2O_4 viewed along the *b*-axis. e) The amplified $[AE_2(B_2O_5)]$ building block analogous to the "Lu-Ban stool" model. The BO_3 triangles and the *AE*—O1 bonds serving as the "planks" and "legs" of the "Lu-Ban stool" are highlighted by purple planes and blue sticks, respectively. Detailed labels of the bonds are displayed in Figure S3 (Supporting Information). In (d) and (e), alkali earth (Ca or Sr), B, and O atoms are represented by blue, dark yellow, and red balls, respectively, and BO_3 groups are represented by red triangles.

clearly validates the "Lu-Ban stool" model for ZLC exploration in nondense materials.

The isomorphic crystal structures of CaB_2O_4 and SrB_2O_4 were first determined by Zachariasen[16] and Kim,[17] respectively. They both crystalize in the orthorhombic *Pbcn* space group. As shown in Figure 1d, all boron atoms are bonded with three oxygen atoms to form BO_3 triangles. By sharing the corner oxygen atoms, the two neighboring BO_3 triangles are connected in the shape of a cross, analogous to the two "planks" comprising the face of the "Lu-Ban stool" (see Figure 1e). The *AE*—O1 bonds (highlighted by bold blue sticks in Figure 1d,e) serve as the legs to support the two "planks" aligned along the *a*-axis. Thus, a "Lu-Ban stool"-like $[AE_2(B_2O_5)]$ building unit is built, and these units are interconnected with each other by sharing the vertex oxygen atoms along the *b*-axis. The $[AE_2(B_2O_5)]$ units are further stacked along the *c*-axis, affording a nondense framework of "Lu-Ban stool"-like structures.

The variations in the refined cell parameters of AEB_2O_4, which were extracted from high-pressure synchrotron XRD experiments between 0 and 8.0 GPa, are plotted in **Figure 2**a,b. During the pressure-applying process, no new XRD peak appears for the AEB_2O_4 compounds (Figure S1, Supporting Information), indicating the absence of a phase transition and demonstrating their high mechanical stability. Clearly, the *a*-axes remain nearly constant and change only by 0.3% (Figure 2a and Table S2, Supporting Information) and −0.4% (Figure 2b and Table S2, Supporting Information) for CaB_2O_4 and SrB_2O_4, and the fitted linear compressibilities are 0.30(7) and 0.00(1) TPa^{-1}, respectively. These linear compressibilities are less than the value of diamond (0.75 TPa^{-1})[9] and osmium (≈0.7 TPa^{-1},[11] the most incompressible material to known). Thus, both CaB_2O_4 and SrB_2O_4 can be categorized as typical ZLC materials. To compensate for the incompression along the *a*-axis, the crystals contract along the other two axes, with compressibilities of 1.38(9) TPa^{-1} along the *b*-axis and 4.93(26) TPa^{-1} along the *c*-axis for CaB_2O_4 and 2.16(11) TPa^{-1} along the *b*-axis and 6.93(16) TPa^{-1} along the *c*-axis for SrB_2O_4.

First-principles simulations of the ZLC behaviors in AEB_2O_4 are also performed (see Figure 2a,b). Based on the geometry optimization calculations for CaB_2O_4 and SrB_2O_4, the calculated compressibilities along the *a*-axis are 0.20(7) and −0.62(6) TPa^{-1} (Table S3, Supporting Information), and the values deduced from the full elastic coefficient tensor calculations are 0.30 and −0.35 TPa^{-1} (Table S5, Supporting Information), respectively. All these calculated values are in very good agreement with the experimental ZLC results. Considering that a tiny modification of the chemical bonds between light boron and oxygen atoms is very difficult to determine through experimental XRD analysis, first-principles simulations thus can provide a reliable path to investigate the ZLC mechanism in AEB_2O_4 in depth. Owing to the similar mechanical behaviors of CaB_2O_4 and SrB_2O_4, CaB_2O_4 is focused on for the elucidation of the ZLC mechanism in AEB_2O_4.

The first-principles structural variations in CaB_2O_4 show that, as mainly depicted in Figure 2c (listed in Table S6, Supporting Information), the fluctuation of B—O bonds from 0 to 8.0 GPa (with an average contraction of 0.4%) is much weaker than that of Ca—O bonds (with an average contraction of 2.0%), confirming the rigidity of BO_3 group. However, under this range of pressures, the dihedral angles between the BO_3 triangles experience drastic rotation and decrease from 18.93° to 16.03° (by 15.3%, Figure 2c and Table S6, Supporting Information). Simultaneously, the tilt angles of the Ca—O1 bond with respect to the *c*-axis increase from 25.62° to 26.06° (by 1.7%), as depicted in Figure 2c. The rotation of the BO_3 groups and the inclination of the Ca—O1 bonds actually lead to the pressure-induced expansion (i.e., the negative linear compressibility) along the *a*-axis. This mechanical effect effectively counterbalances the contraction (i.e., the positive linear compressibility) originating from the reduction in the Ca—O1 bond lengths from 2.332 to 2.285 Å (by 2.01%) under the exerted hydrostatic pressure from 0 to 8.0 GPa. As a result, ZLC behavior occurs in CaB_2O_4 because the contraction of the Ca—O1 "legs" along the *a*-axis subtly balances the expansion owing to the decrease in the dihedral angles between the BO_3 "planks" and the inclination of the Ca—O1 "legs" with respect to the *c*-axis in the "Lu-Ban stool"-like $[Ca_2(B_2O_5)]$ microscopic structures (Figure 2d). The same conclusion can be deduced for SrB_2O_4 (see the data listed in Figure S4 and Table S6, Supporting Information). In fact, the Poisson's ratios obtained from the first-principles elastic constants indicate that the $\nu_{12} + \nu_{13}$ values approach 1 for both CaB_2O_4 (0.966) and SrB_2O_4 (1.043), thereby satisfying the criterion for the ZLC effect in nondense materials. In particular, the fact that $\nu_{13} >> \nu_{12}$ (see Table S5, Supporting Information) demonstrates that the ZLC behavior in both materials originates from a quasi-2D mechanical mechanism.

Notably, the ZLC magnitude in CaB_2O_4 is slightly larger than that in SrB_2O_4. According to the architect of the Lu-Ban stool, the pressure-induced rotation of the planks is tightly correlated with the inclination of the legs; therefore, modification of the legs is one of the principle sources of the ZLC behavior. Detailed analysis reveals that the small mechanical difference between CaB_2O_4 and SrB_2O_4 is mainly attributable to the bond character in the *AE*—O1 bonds and the rotation of the BO_3 groups. Figure 2e illustrates the first-principles electron density difference maps of the *AE*—O1 bonds in CaB_2O_4 and SrB_2O_4. Clearly, a considerable amount of charge density (mainly from the Ca 4s electrons) redistributes from off-bond to the near-bond area of the Ca—O1 bond in CaB_2O_4 (upper panel in Figure 2e). In comparison, almost all the Sr 5s electrons are transferred to the oxygen atoms as the Sr—O1 bond forms, leaving a near-spherical distribution of an electron-deficient area around the Sr atoms in SrB_2O_4 (lower panel in Figure 2e). This finding highlights that the Ca—O1 bonds have a stronger covalent character than the Sr—O1 bonds, which was also confirmed by quantitative Mulliken population calculations[19] (M = 0.14 and 0.10 for Ca—O1 and Sr—O1, respectively. A larger Mulliken population M indicates a bond with a stronger covalent nature). The strong directivity of covalent bonds makes the inclination of the Ca—O1 bonds smaller than that of the Sr—O1 bonds as the pressure increases (see Table S6, Supporting Information). This leads to the BO_3 "planks" in CaB_2O_4 experiencing less rotation than those in SrB_2O_4 (see Table S6, Supporting Information). Since both the inclination of the *AE*—O1 bonds and the rotation between the BO_3

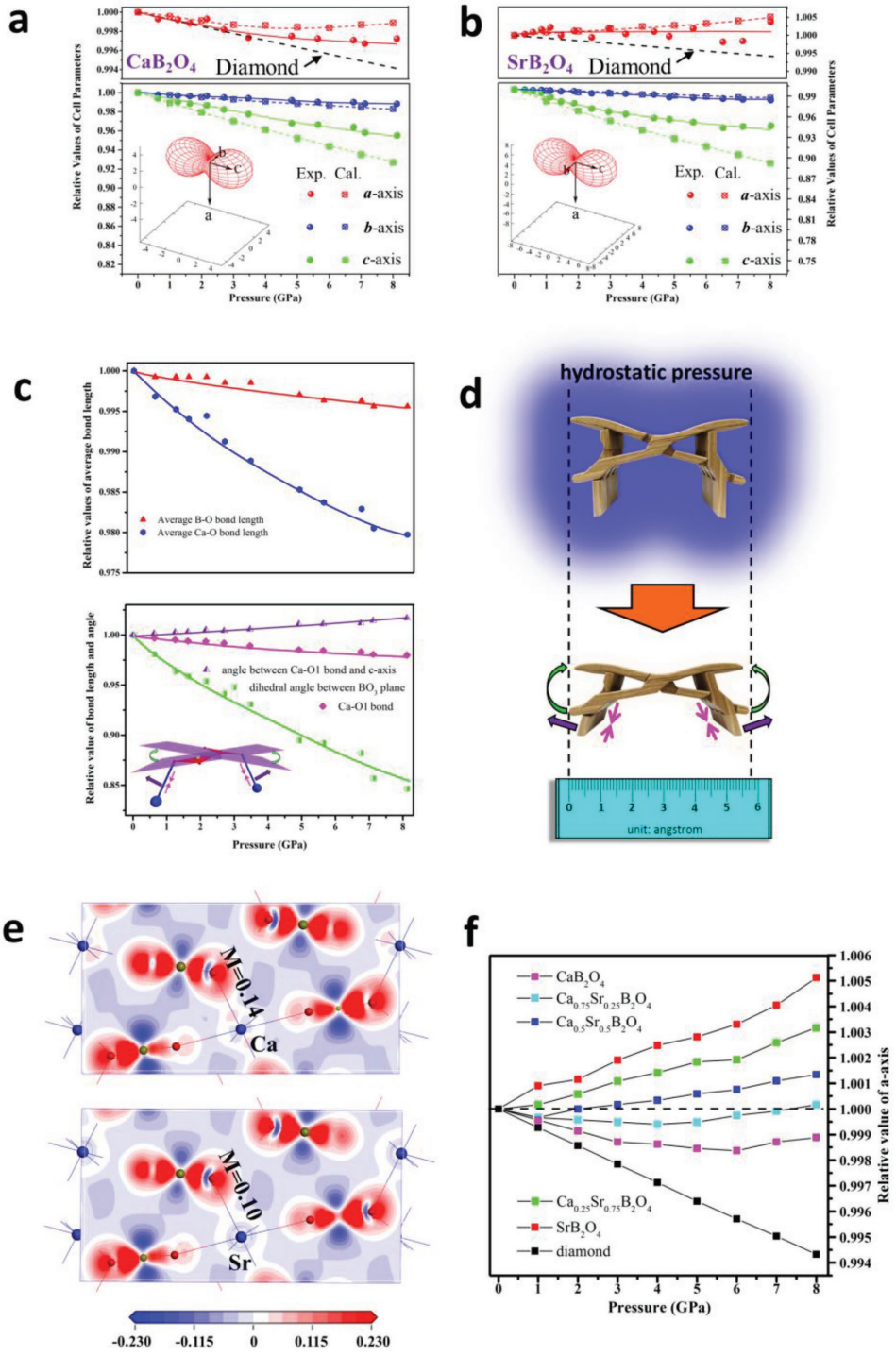

Figure 2. ZLC behaviors and ZLC mechanism in AEB_2O_4. a,b) Experimental and first-principles results for the variation in cell parameters of CaB_2O_4 and SrB_2O_4 with respect to pressure. The insets are the orientation distributions of compressibility generated by PASCAL program[18] based on the experimental cell parameters. The cell variations of diamond are plotted by dashed lines according to the fitted equation of states in ref. [9]. c) The variations in average B—O and Ca—O bond lengths (upper panel) and the main modifications of the "Lu-Ban stool"-like structure (lower panel) in CaB_2O_4 with respect to pressure. The green arrows indicate the decrease in dihedral angles between the BO_3 "planks," the violet arrows indicate the inclination of the Ca—O1 "legs" with respect to the *c*-axis, and the pink arrows indicate the contraction of the Ca—O1 "legs". d) Schematic of the ZLC behavior in AEB_2O_4. e) Electron density difference maps of CaB_2O_4 (upper panel) and SrB_2O_4 (lower panel). *M* denotes Mulliken population. f) Variation in the calculated cell parameters of $Ca_xSr_{1-x}B_2O_4$ with respect to pressure. The calculated cell parameters of diamond with the same computational parameters are also plotted for comparison. Based on the calculated cell parameters, the fitted linear compressibility of diamond is 0.71 TPa^{-1}, which is in good agreement with the experimental value (0.75 TPa^{-1}).

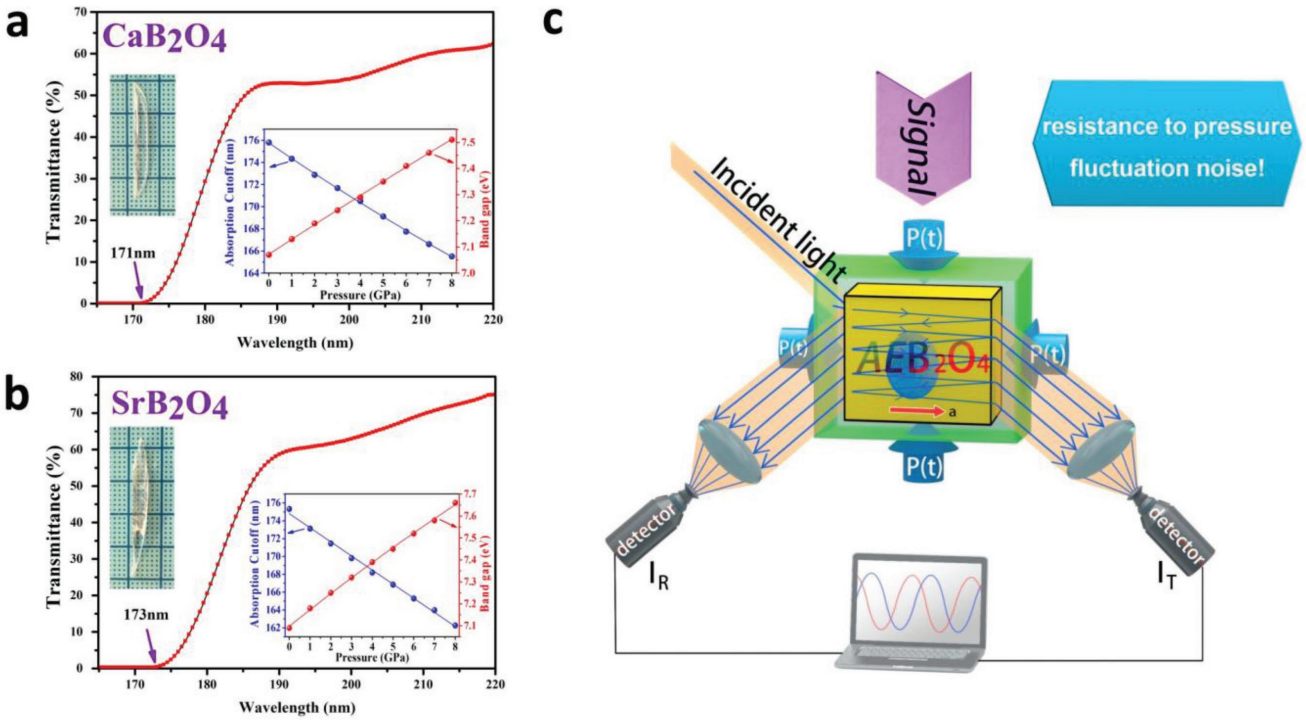

Figure 3. A proposed application of the ZLC behavior in AEB_2O_4. a,b) Transmittance spectra of CaB_2O_4 and SrB_2O_4, respectively. The inset displays the as-grown crystals and variation in the theoretical absorption edges and bandgaps as function of pressure. c) Schematic of an application of AEB_2O_4 to an ultrafine optical instrument operated in a pressure-fluctuating environment. Here, the input signals include those correlated with temperature, voltage, displacement, etc.

triangles result in the pressure-induced expansion, the smaller contribution of this effect in CaB_2O_4 causes it to exhibit more positive linear compressibility than SrB_2O_4 (0.30(7) TPa^{-1} for CaB_2O_4 versus 0.00(1) TPa^{-1} for SrB_2O_4 from 0 to 8.0 GPa). Because CaB_2O_4 and SrB_2O_4 have the same isomorphism, it is anticipated that the ZLC magnitude in the solid solution between CaB_2O_4 and SrB_2O_4, that is, $Ca_xSr_{1-x}B_2O_4$ (x = 1 to 0), can be tailored, as confirmed by our first-principles simulations (see Figure 2f and Table S3, Supporting Information). This implies that their use in practical applications would be more convenient.

The deep-UV transmittance spectral measurements revealed that CaB_2O_4 and SrB_2O_4 exhibit an absorption edge of 171 and 173 nm, respectively (corresponding to bandgaps of 7.27 and 7.18 eV, respectively, **Figure 3**a,b). Meanwhile, the first-principles calculations demonstrated that the bandgaps of both materials increase as the pressure increases from 0 to 8.0 GPa. This result indicates that the wide bandgaps (i.e., short absorption edges) can also be well maintained under high pressure (as depicted in the inset in Figure 3a,b and listed in Table S7, Supporting Information). The bandgaps for AEB_2O_4 are significantly larger than that of diamond (≈5.5 eV[20]), the best material for the optical devices under high-pressure environments. Thus, AEB_2O_4 can be used in the optical apparatus adopting deep-ultraviolet laser such as argon fluoride excimer laser with the wavelength of 193 nm, where diamond is inapplicable.

Considering that the precision and resolution of an optical instrument are closely dependent on its working waveband, the combination of ZLC behavior and good optical transmittance provided by the AEB_2O_4 compounds with wide bandgaps should promote their use in some unique but important applications in advanced optical instruments operated in pressure-fluctuating environments, as schematically depicted in Figure 3c. In this proposed optical apparatus, AEB_2O_4 can serve as an ultrafine sensor device to monitor the signals from the surrounding environment: temperature, voltage, displacement, etc. Such signals can lead to changes in the optical length in an optical material, which in turn can be detected from the interference patterns. When our proposed optical apparatus is operated in a pressure-fluctuating environment, the constant size along the ZLC direction (along the *a*-axis) would eliminate the influence of pressure fluctuation on the optical length. Thus, the disturbance from environmental pressure noise can be effectively avoided, and the signals can be precisely detected. This advanced optical instrument, therefore, would have important applications in ultrastable optical telecommunication devices in deep sea,[1,4] and ultrastable optical transmittance windows in monitor or sensor devices in submarines and aerocrafts.[7]

Moreover, owing to the ZLC behavior the acoustic velocities in AEB_2O_4 are highly anisotropic, with the ratio between the highest and lowest velocities up to 4:1 (see Table S8, Supporting Information). The low acoustic velocities would make AEB_2O_4 a suitable medium material in acoustic-optics apparatus to improve the acoustic-optics coupling efficiency,[21] such as in acoustic-optics modulator, acoustic-optics diffractometer, and acoustic-optics filter.[22] Meanwhile, the high acoustic velocities

in AEB_2O_4 could be used in acoustic wave propagating devices to improve the response speed, such as in acoustic lens and for phononic crystals fabrication. In addition, both CaB_2O_4 and SrB_2O_4 can be synthesized in open environments, which would considerably simplify their practical application and commercial manufacture.

In summary, associated with the "Lu-Ban stool" structure obtained from traditional Chinese woodworking, we propose an analogous model that can effectively stop the compression in nondense materials. With this model, the very rarely observed ZLC effects were discovered in AEB_2O_4 (AE = Sr or Ca) in the hydrostatic pressure range from 0 to 8.0 GPa through high-pressure XRD experiments. First-principles calculations demonstrated that the ZLC behavior can be mainly attributed to the subtle counterbalance between the expansion effect from the rotation of the BO_3 "planks" in conjunction with the inclination of the AE—O1 "legs" and the contraction effect from the shrinkage of the AE—O1 "legs" in the "Lu-Ban stool" under hydrostatic pressure. Based on the established effect of the "Lu-Ban stool"-like structure, the ZLC behavior in the AEB_2O_4 material system can definitely be tailored. Coupled with the wide bandgap, the ZLC behavior in AEB_2O_4 may encourage its widespread applications in ultraprecise scientific and engineering instruments used in high-pressure fluctuating environments or for pressure-detecting purposes. We believe that the explorations based on the "Lu-Ban stool"-like structure will open a new avenue in the search for and design of novel ZLC materials and will eventually stimulate continuous discoveries of this fascinating mechanical behavior with great prospective applications.

Supporting Information

Supporting Information is available from the Wiley Online Library or from the author.

Acknowledgements

X.J., Y.Y., and M.M. contributed equally to this work. The authors acknowledge Zhuohong Yin for useful discussions. This work was supported by the National Scientific Foundations of China (Grant Nos. 11474292, 51702330, 11611530680, 91622118, and 91622124), Russian Foundation for Basic Research (Grant No. 17-52-53031), the Special Foundation of the Director of Technical Institute of Physics and Chemistry (TIPC), the China "863" project (No. 2015AA034203), key project of Beijing Synchrotron Radiation Facility and the Youth Innovation Promotion Association, CAS (outstanding member for Z.L. and Grant No. 2017035 for X.J.).

Conflict of Interest

The authors declare no conflict of interest.

Keywords

borates, "Lu-Ban stool"-like structure, ultraviolet transparency, zero linear compressibility

Received: February 27, 2018
Revised: May 9, 2018
Published online: June 25, 2018

[1] R. H. Baughman, S. Stafstrom, C. X. Cui, S. O. Dantas, *Science* **1998**, *279*, 1522.
[2] A. B. Cairns, J. Catafesta, C. Levelut, J. Rouquette, A. van der Lee, L. Peters, A. L. Thompson, V. Dmitriev, J. Haines, A. L. Goodwin, *Nat. Mater.* **2013**, *12*, 212.
[3] a) J. N. Grima, R. Caruana-Gauci, *Nat. Mater.* **2012**, *11*, 565; b) W. Cai, A. Katrusiak, *Nat. Commun.* **2014**, *5*, 4337.
[4] R. H. Baughman, *Nature* **2003**, *425*, 667.
[5] a) J. B. Berger, H. N. G. Wadley, R. M. McMeeking, *Nature* **2017**, *543*, 533; b) J. J. do Rosario, E. T. Lilleodden, M. Waleczek, R. Kubrin, A. Y. Petrov, P. N. Dyachenko, J. E. C. Sabisch, K. Nielsch, N. Huber, M. Eich, G. A. Schneider, *Adv. Eng. Mater.* **2015**, *17*, 1420; c) Y. Tian, B. Xu, D. Yu, Y. Ma, Y. Wang, Y. Jiang, W. Hu, C. Tang, Y. Gao, K. Luo, Z. Zhao, L.-M. Wang, B. Wen, J. He, Z. Liu, *Nature* **2013**, *493*, 385; d) J. Bauer, A. Schroer, R. Schwaiger, O. Kraft, *Nat. Mater.* **2016**, *15*, 438; e) Q. Li, Y. Ma, A. R. Oganov, H. Wang, H. Wang, Y. Xu, T. Cui, H.-K. Mao, G. Zou, *Phys. Rev. Lett.* **2009**, *102*, 175506.
[6] H.-Y. Chung, M. B. Weinberger, J. B. Levine, A. Kavner, J.-M. Yang, S. H. Tolbert, R. B. Kaner, *Science* **2007**, *316*, 436.
[7] A. Witze, *Nature* **2017**, *546*, 466.
[8] A. L. Goodwin, D. A. Keen, M. G. Tucker, *Proc. Natl. Acad. Sci. USA* **2008**, *105*, 18708.
[9] F. Occelli, P. Loubeyre, R. Letoullec, *Nat. Mater.* **2003**, *2*, 151.
[10] H. Liu, W. A. Caldwell, L. R. Benedetti, W. Panero, R. Jeanloz, *Phys. Chem. Miner.* **2003**, *30*, 582.
[11] H. Cynn, J. E. Klepeis, C. S. Yoo, D. A. Young, *Phys. Rev. Lett.* **2002**, *88*, 135701.
[12] H. Gou, N. Dubrovinskaia, E. Bykova, A. A. Tsirlin, D. Kasinathan, W. Schnelle, A. Richter, M. Merlini, M. Hanfland, A. M. Abakumov, D. Batuk, G. Van Tendeloo, Y. Nakajima, A. N. Kolmogorov, L. Dubrovinsky, *Phys. Rev. Lett.* **2013**, *111*, 157002.
[13] D. Maspoch, D. Ruiz-Molina, J. Veciana, *Chem. Soc. Rev.* **2007**, *36*, 770.
[14] a) J. Haines, C. Chateau, J. M. Leger, C. Bogicevic, S. Hull, D. D. Klug, J. S. Tse, *Phys. Rev. Lett.* **2003**, *91*, 157002; b) R. S. Bubnova, S. K. Filatov, *Z. Kristallogr. – Cryst. Mater.* **2013**, *228*, 395.
[15] C. T. Chen, T. Sasaki, R. K. Li, Y. C. Wu, Z. S. Lin, Y. Mori, Z. G. Hu, J. Y. Wang, G. Aka, M. Yoshimura, Y. Kaneda, *Nonlinear Optical Borate Crystals: Principles and Applications*, Wiley-VCH, Weinheim, Germany **2012**.
[16] W. H. Zachariasen, G. E. Ziegler, *Z. Kristallogr.* **1932**, *83*, 354.
[17] J. B. Kim, K. S. Lee, I. H. Suh, J. H. Lee, J. R. Park, Y. H. Shin, *Acta Crystallogr., Sect. C: Cryst. Struct. Commun.* **1996**, *52*, 498.
[18] M. J. Cliffe, A. L. Goodwin, *J. Appl. Crystallogr.* **2012**, *45*, 1321.
[19] R. S. Mulliken, *J. Chem. Phys.* **1955**, *23*, 1833.
[20] C. Kittel, *Introduction to Solid State Physics*, Wiley, New York **2004**.
[21] X. Jiang, S. Luo, L. Kang, P. Gong, W. Yao, H. Huang, W. Li, R. Huang, W. Wang, Y. Li, X. Li, X. Wu, P. Lu, L. Li, C. Chen, Z. Lin, *Adv. Mater.* **2015**, *27*, 4851.
[22] P. F. Tian, D. Keusters, Y. Suzaki, W. S. Warren, *Science* **2003**, *300*, 1553.

